STRUCTURAL ANALYSIS OF MICROCLUSTERS

BY

CLASSICAL AND QUANTUM MECHANICAL MINIMIZATION METHODS

A MASTER'S THESIS

IN

CHEMISTRY

MIDDLE EAST TECHNICAL UNIVERSITY

BY

NURAN ELMACI

SEPTEMBER 1990

to my mother

Approval of Graduate School of Natural and Applied Sciences.

Prof.Dr.Atpay ANKARA
Director

I certify that this thesis satisfies all the requirements as a thesis for the degree of Master of Science in Chemistry.

Prof.Dr.Namık K.ARAS
Chairman of the Department

We certify that we have read this thesis and that in our opinion it is fully adequate, in scope and quality, as a thesis for the degree of Master of Science in Chemistry.

Prof.Dr.Ersin YURTSEVER
Supervisor

Examining Comittee in Charge:

Prof.Dr.H.Önder PAMUK (Chairman)

Prof.Dr.Ural AKBULUT

Prof.Dr.Şefik SÜZER

Prof.Dr.Ersin YURTSEVER (Supervisor)

Prof.Dr.İlker ÖZKAN

ii

ABSTRACT

STRUCTURAL ANALYSIS of MICROCLUSTERS by
CLASSICAL and QUANTUM MECHANICAL MINIMIZATION METHODS

ELMACI, Nuran

M.S. in Chemistry

Supervisor: Prof.Dr.Ersin YURTSEVER

September 1990   Pages: 60

In this work, structural analyses of microclusters arecarried out by using classical and quantum mechanical minimization methods. For the classical calculations, optimization of the total energy is achieved with two-body potential functions as usual. Then effects of the three-body forces to these structures are analyzed. The same set of high-symmetry clusters made of Carbon atoms are studied by a semi-empirical quantum mechanical method (AM1).

At large three-body intensity parameter Z^*, both AM1 and static results show that linear conformations are preferred to two-dimensional structures. Three-dimensional structures seem to be the least stable ones. But at small Z^*, these results are reversed. Overall there is a good agreement between both set of results for $Z^*=0.8$, suggesting that a qualitative analysis of Carbon clusters can be done with simple potential functions provided that properly weighted three-body interactions are also employed.

Key-Words: Clusters, Optimization, Lennard-Jones, Axilrod-Teller, AM1

Science Code: 405.04.01

ÖZET

KLASİK VE KUANTUM MEKANİK MİNİMİZASYON METODLAR YOLUYLA MİKROKLUSTERLARIN YAPISAL ANALİZİ

ELMACI, Nuran

Yüksek Lisans Tezi, Kimya

Tez Yöneticisi: Prof.Dr. Ersin Yurtsever

Eylül 1990

Bu çalışmada Klasik ve Kuantum mekanik enerji minimizasyon yöntemleri kullanılarak mikroklusterların yapısal analizleri araştırıldı. Klasik hesaplarda, toplam enerji, ikili etkileşimler kullanılarak optimize edildi. Daha sonra üçlü etkilesim etkileri incelendi. Aynı yüksek simetri yapıları, karbon klusterları için, yarı-deneysel kuantum method AM1, kullanılarak çalışıldı.

Üçlü etkileşim parametresinin (Z^*) büyük olduğu bölgelerde, AM1 ve Statik sonuçları, lineer yapıların iki-boyutlu yapılara tercih edildiklerini gösterdi. Üç-boyutlu yapıların en kararsız yapılar olduğu görüldü. Fakat küçük Z^* de bu sonucun tersi gozlendi. Genel olarak $Z^*=0.8$ için, her iki yöntemin sonuçlarında iyi bir uyum olduğu saptanmıştır. Buna dayanarak, basit potensiyel fonksiyonlarının yanısıra üçlü etkileşmeler de katılarak karbon klusterları için nitel analiz yapılabileceği önerilmistir.

Anahtar kelimeler: Klusterlar, Optimizasyon, Lennard-Jones, Axilrod-Teller, AM1

ACKNOWLEDGEMENTS

v

TABLE OF CONTENTS

LIST OF TABLES

LIST OF FIGURES

INTRODUCTION

1.1 Scope and Objective

The last fifteen years have seen an explosion of clusters research brought about two relatively new experimental advances , supersonic jet expansions creating cold high density atomic and molecular beams, and laser (mass and optical) spectroscopy. The dictionary meaning of a cluster is a number of similar things growing together or persons collected or grouped closely together. Hoare [1] defined clusters as aggregates of whether atoms, molecules, ions etc. so small that an appreciable proportion of these units must be present on its surface at any given time. Halıcıoğlu and his collaboraters [2] defined them as aggregates held under different conditions. Also Brickmann and Polymeropoulos [3] used the definition as aggregates in which each atom is not farther away than a distance 2.0 σ from at least one other atom, where σ is the hard-sphere diameter.

Classification of clusters can be made according to many things, such as their compositions, sizes, surroundings etc. In general very small clusters are defined as those containing 2-10 atoms; and small size clusters are those with

1

10-10^{2}atoms; medium size, large size and very large clusters containing 10^2-10^3, 10^3-10^4, more than 10^5 respectively [2].

In the last decade, there is a remarkable increase in the study of microclusters physics and chemistry. These fields are nucleation process, crystal growth, epitaxy, catalysis and photographic chemistry effected by previously separated fields. The properties of microclusters are different than their bulk properties. For example the average number of nearest neighbors of an atom in the bulk phase means its chemical valence but in a cluster, it is not so well-defined [4]. Also many quantities (temperature, surface tension etc.) that are used to describe macroscopic systems can not be used for a description of microscopic systems. Because of these factors , the standard methods cannot be used in the study of microscopic systems.

Another important area of the study of microclusters is the astrophysical theories where small interstellar grains are used in the regulation of hydrogen equilibria in the galaxy. Superconductivity, ferromagnetism and structural stability of clusters (or magic numbers), electronic properties of clusters can be considered among the theoretical problems in the field of cluster research.

Many attempts have been made to predict the energetically most favorable structures of small clusters

[5-14]. Calculations of this sort may be classified into three groups:

i) Quantum mechanical calculations which are based on either ab-initio or semi-empirical methods.

ii) Simulation studies which may be classified in to Molecular Dynamics and Monte Carlo or static methods.

Ab-initio methods are based on self-consistent field approach in which all necessary integrals are computed analytically. Although these methods give very accurate results for small molecules, the calculations become extremely difficult with the increasing system size.

In the quantum-mechanical semi-empirical methods, the same integrals are calculated by incorporating some parameters either adjusted to fit experimental data, or results from ab-initio calculations. There are two kinds of semi-empirical methods; one using one electron Hamiltonian only and the other relying on parametrical functions to approximate the full two-electron Hamiltonian. An example for the first one is Hückel molecular orbital theory which is mostly used in the study of conjugated hydrocarbons. This

method uses a one-electron hamiltonian and takes the bond integrals as adjustable parameters rather than quantities to be calculated theoretically. The most common examples for the second type of semi-empirical methods are MINDO/3,MNDO and AM1 [15-17]. These methods are useful for obtaining molecular geometries, heat of formation, etc. especially for organic compounds.

In the study of small clusters ,computer simulation techniques based on the atomistic considerations provide a useful approach. Molecular Dynamics and Monte Carlo methods are the two common atomic level computer simulation methods

In Molecular Dynamics technique the classical equations of motion are solved numerically for grouped N-atom clusters. Generally this method uses microcanonical ensemble (N,V,E). The atomic coordinates and their time derivatives representing the system's motion (motion of every atom) are generated as time-order series. The temperature effects are included intrinsically in the result by incorporation of kinetic energies with the calculation scheme. With a sufficient number of iterations Molecular Dynamics calculations can simulate any time-dependent (non-equilibrium) as well as equilibrium quantity [2].

Monte Carlo techniques in general are based on the canonical ensemble (N,V,T). For initial coordinates the atoms

in the cluster are randomly placed in a unit cell. Then each particle is moved for a large number of times and the outcome of these moves are based on some probabilistic formulas. After sufficient number of iterations the desired quantities are calculated as ensemble averages from position dependent quantities estimated in every step. Any equilibrium quantity can be calculated as a function of temperature [2].

The static method is based on a simple minimization technique to find the configuration of a cluster corresponding to a hopefully global energy minimum. It is a temperature independent approach and can be regarded as the T=0 K case. Because of the simplicity of the static method and its small demand on the computation time, it is used quite frequently to obtain optimum points. However one must be careful in identification of these points, since there usually are a large number of local minima [2].

All three of these methods rely on some type of a potential energy function which describes the total interaction energy among atoms as functions of their positions in the cluster. For computational reasons, it is necessary to define the total potential energy of the system in terms of parametrical functions.

If it is assumed that a function, $\Phi(\vec{r}_1, \vec{r}_2, \ldots, \vec{r}_N)$ exists to describe the total potential energy of an isolated

system of N atoms as a function of their positions, then
without any loss of generality the function Φ can be expanded
as;

$$\Phi = \sum_{\substack{i \\ i<j}}^{N} \sum_{j}^{N} u(\vec{r}_i, \vec{r}_j) + \sum_{\substack{i \\ i<j<k}}^{N} \sum_{j}^{N} \sum_{k}^{N} u(\vec{r}_i, \vec{r}_j, \vec{r}_k) + \ldots\ldots$$

$$+ \sum_{\substack{i \\ i<j<..<n}}^{N} \ldots\ldots\ldots \sum_{r}^{N} u(\vec{r}_i, \vec{r}_j, \ldots \vec{r}_n) + \ldots\ldots \qquad (1.1)$$

where $u(\vec{r}_i, \vec{r}_j)$, $u(\vec{r}_i, \vec{r}_j, \vec{r}_k)$ and $u(\vec{r}_i, \ldots, \vec{r}_n)$ denote the two
body ,three body and n-body expansion of Φ. It is usually
believed that the series has a rapid convergence, therefore
the higher moments may be neglected. Otherwise the equation
is too cumbersome to be employed for systems containing more
then only a few atoms.

In the simplest approach the three-body and higher
terms are neglected and the potential energy is represented
only by a pair potential. This approximation is called
first-order approximation and may be useful in the
thermodynamical study and the rare gase clusters where the
role of many-body forces are minimal [18]. However one of the
recent studies indicates that even though for rare gases
there is influence of three-body forces. It is shown that for
xenon cluster there is a magic number "13", but for argon

6

there is none, due to the three-body dispersion (triple-dipole) forces which are related to the polarizability [19]. Polarizability of xenon is 2.5 times larger than that of argon. Three-body contribution increases with increasing covalent character.

More recent studies indicate the importance of three-body forces in cluster research [20-28]. Halıcıoğlu and White [20] calculated micro-cluster shapes with addition of three-body forces to the energy. They concluded that linear and two dimensional structures are preferred to three dimensional structures. Also Öksüz [26] showed that, for 13 atom clusters, pentagonal pyramid and tetrahedral shapes can be energetically preferred depending on the strength of three-body forces instead of icosahedron which is the most stable structure if only two-body potential was considered [1].

The origin of all the forces between atoms and molecules is the interactions of permanently or temporarily charged particles. These interactions are usually expressed as $(Q_1 Q_2 r^{-n})$. Q_1, Q_2 are charges of interacting particles and the magnitude of n determines whether it is a short- or long-range interaction.

Short-range interactions are called valence or chemical forces. They become important when the particles come

together close enough for their electron clouds to overlap. The long-range interactions can be considered in three parts; electrostatic, induction and dispersion. These contributions arise from various types of interactions. A direct application of Coulombic law of electrostatic interaction is the most general one ($U \propto r^{-1}$). In the induction effect a charged particle (or an ion) interacts with a neutral molecule ($U \propto r^{-4}$). Dispersion forces are important for the interactions between nonpolar molecules. These type of interactions are also called London Forces(induced dipole-induced dipole) ($U \propto r^{-6}$) [29].

In general, a potential function which describes the interaction of a diatomic system must obey the following conditions;

1) $u(r_{ij}) \longrightarrow 0$ as $r \longrightarrow \infty$

2) $u(r_{ij}) \longrightarrow \infty$ for $r < r_{min}$ and $r_{min} \geq 0$

3) $u'(r_{ij}) \longrightarrow = 0$ for a unique r_0 with $r_{min} < r_0 < \infty$

4) $u''(r_0) > 0$ and $u(r_0) < 0$

The most common pair potentials are,

1) $u(r_{ij}) = (m-n) [nr^{-m} - mr^{-n}]$ (Mie)

2) $u(r_{ij}) = r^{-6} - 2r^{-12}$ (Lennard Jones)

3) $u(r_{ij}) = [1 - e^{\alpha(1-r)}]^2 - 1$ (Morse)

4) $u(r_{ij}) = Ae^{-ar^2} - Be^{-br^2}$ (Gaussian)

5) $u^{\alpha\beta}(r_{ij}) = 2^{\alpha}2^{\beta}/r + Ae^{-r/\rho}$ (Born-Mayer)

8

They all satisfy the first condition. The condition
(2)is satisfied by 1,2,5 but not by 3 and 4. But then some
artificial cutoff can be introduced such that $u(r_{ij})=\infty$ if r_{ij}
$\leq r_{cut}$ [1].

The purpose of this work is to analyze a number of
energetically favorable structures of clusters up to
six-atoms by direct minimization of the total energy .The
effect of three-body forces on the structure of these
microclusters are investigated. For carbon clusters,
comparison of the results with a semi-empirical quantum
mechanical method (AM1) is also carried out.

2.1. Potential Functions

A Lennard-Jones type pair potential was chosen as the two-body part of the total energy.

$$u(r_{ij}) = 4\varepsilon\left[\left(\frac{\sigma}{r_{ij}}\right)^{12} - \left(\frac{\sigma}{r_{ij}}\right)^{6}\right] \qquad (2.1)$$

where σ is the hard-sphere diameter, r_{ij} is the distance between i'th and j'th atoms, ε is the energy at equilibrium separation distance(depth of the potential well).
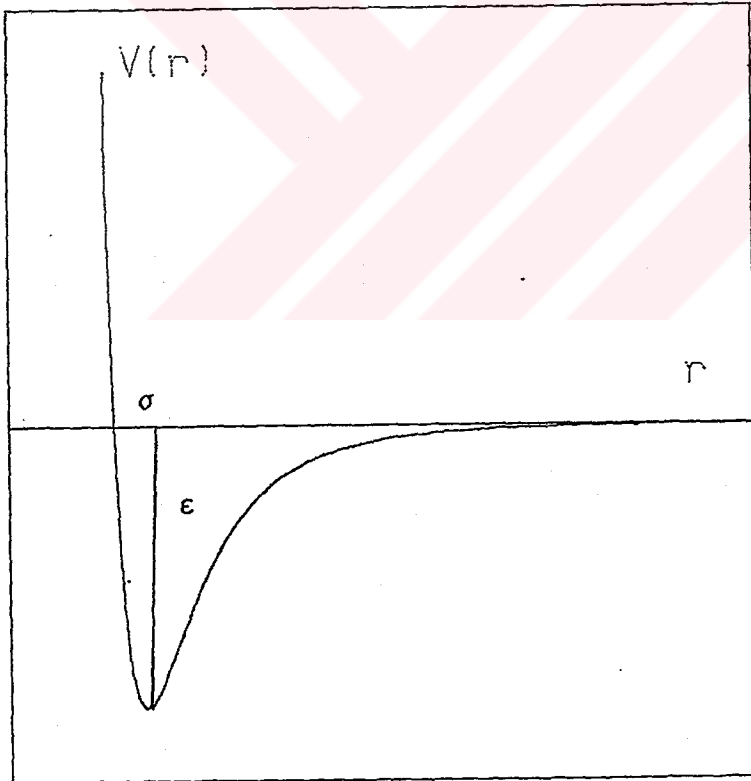
Figure 1. Lennard-Jones (LJ) pair potential.

$\left[\dfrac{\sigma}{r_{ij}}\right]^{12}$ term is the short range repulsive term. At small r values repulsive part is predominant.

$-\left[\dfrac{\sigma}{r_{ij}}\right]^{6}$ term is the long range attraction part of the potential. At large separations the attractive part is predominant. This term represents dispersion forces, induced dipole -induced dipole type interactions.

If two parts of the potential are drawn separately,
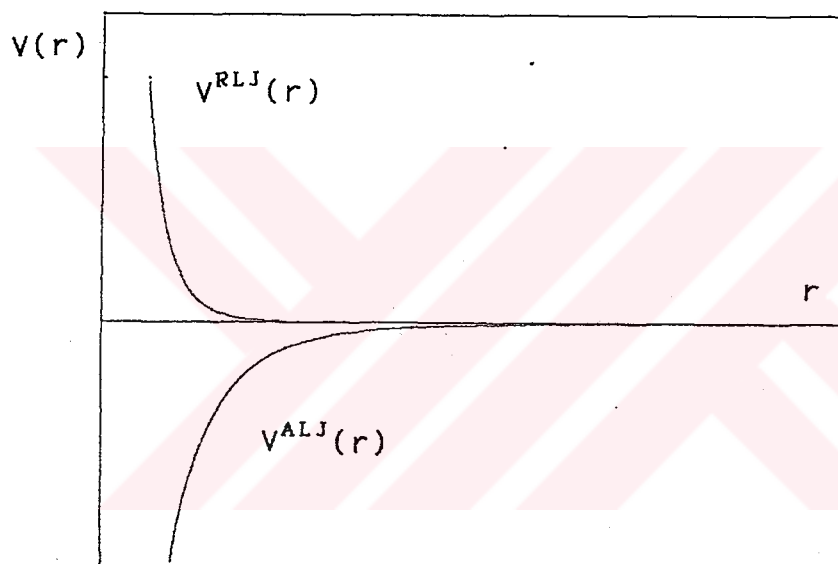
Figure 2. Attractive and repulsive components of LJ.

This function gives a very simple realistic representation for the interaction of spherical non-polar molecules [30].

By applying perturbation theory up to second order, the dispersion potential ($V \propto \dfrac{1}{r^6}$) between two nonpolar particles can be obtained. Similarly the three-body dispersion potential between triplets can be derived by applying Rayleigh-Schrodinger perturbation theory up to third order.

The three body dispersion potential was first obtained by Axilrod-Teller [31-33]. The so called Axilrod-Teller triple-dipole potential is,

$$u(\vec{r}_i, \vec{r}_j, \vec{r}_k) = Z \left[\frac{(1+3Cos\theta_i Cos\theta_j Cos\theta_k)}{(r_{ij} r_{ik} r_{jk})^3} \right] \qquad (2.2)$$

Where $\theta_i, \theta_j, \theta_k$ and r_{ij}, r_{jk}, r_{ik} represent the angles and the sides of the triangle formed by the three particles i,j,k respectively. The three-body intensity parameter is denoted by Z.

This potential represents the long-range dispertial interactions. The intensity parameter is proportional to the ionization potential and third power of the polarizability.

$$Z = \frac{9}{16} I\alpha^3 \qquad (2.3)$$

The sign of the term $(1+3Cos\theta_i Cos\theta_j Cos\theta_k)$ depends on configuration of atoms;

1) If all three angles < 90° it is positive (repulsive potential).

2) If one angle > 90° it is negative (attraction)

3) If three atom are placed in a straight line (linear),it takes a minimum value (-2) which indicates a strong attraction.

2.2. Scaling of the Parameters

The parameters of potential can be reduced by appropriate scaling. The total energy is,

$$U= \sum_{i=2}^{N} \sum_{j=1}^{i-1} 4\varepsilon \left[\left[\frac{\sigma}{r_{ij}} \right]^{12} - \left[\frac{\sigma}{r_{ij}} \right]^{6} \right] +$$

$$\sum_{i=3}^{N} \sum_{j=2}^{i-1} \sum_{k=1}^{j-1} Z \left[\frac{(1+3\cos\theta_i \cos\theta_j \cos\theta_k)}{(r_{ij} r_{ik} r_{jk})^3} \right] \qquad (2.4)$$

If we define,

$$r_{ij}^* = \frac{r_{ij}}{\sigma} \quad ; \quad U^* = \frac{U}{4\varepsilon} \quad ; \quad Z^* = \frac{Z}{4\varepsilon\sigma^9}$$

then the final dimensionless potential becomes,

$$U^* = \sum_{i=2}^{N} \sum_{j=1}^{i-1} \left[\left[\frac{1}{r_{ij}^*} \right]^{12} - \left[\frac{1}{r_{ij}^*} \right]^{6} \right] +$$

$$\sum_{i=3}^{N} \sum_{j=2}^{i-1} \sum_{k=1}^{j-1} Z^* \left[\frac{(1+3\cos\theta_i \cos\theta_j \cos\theta_k)}{(r_{ij}^* r_{ik}^* r_{jk}^*)^3} \right] \qquad (2.5)$$

13

2.3. Optimization

The solution of $\dfrac{\delta E}{\delta q_i}=0$ for i=1,...3N-6 provide the optimum points of the potential hypersurface .These optimum points can be characterized by their second derivatives. For functions of only one variable, the first derivative is zero at a minimum, maximum or an inflection point. At a minimum point, second derivative is positive, at a maximum its value is negative, and at an inflection, its value is zero. For functions with more than one variable, gradient is defined as the first derivative vector with respect to all variables. The second derivative matrix is called Hessian. For optimum points the first derivatives with respect to all variables must be smaller than a given threshold Δ, that is the gradient vector must have zero length.

The first derivative of potential energy for a system gives forces acting on the system and the second derivatives give force constants. So if the gradient vector is zero the molecule is in a stationary position. Hessian matrix is then used to characterize these points. If all eigenvalues of hessian are positive, it corresponds to a local minimum, if they are all negative it is a local maximum. The saddle point may be defined as first order,second order etc. If there is one negative eigenvalue it is called a first order saddle

14

point. It is a maximum in one variable and minimum in all others. If there are n negative eigenvalues , it is a n^{th}order saddle point. A zero eigenvalue indicates inflection point.

In the optimization process, the important points are the choice of coordinates and the starting geometry. The gradient and hessian may be computed analytically or numerically based on some approximate schemes.

The coordinates can be chosen as internal or cartesian coordinates. Internal coordinates contain bond length, valence and dihedral angles. Internal coordinates are usually preferred,since the total energy is invariant for overall translation and rotation. There is one transformation from internal to cartesian coordinates but there may be more than one for the reverse case. Even though the internal coordinates are not unique , one must be careful to obtain a chemically reasonable set. The coordinates must describe the system uniquely.

There are many methods of optimization. They may use only the function or function plus gradient or function, gradient, hessian. The problem is the calculation of hessian and gradient matrices.

The steps in optimization are;

1) Starting with a geometry X_k, initially k=0, hessian

and its inverse are estimated.

2) The energy (E_k) for X_k and gradient (g_k) is calculated.

3) Hessian is updated, so that the model surface fits the current energy and the gradient as well as from previous steps (omit for the first point).

4) The minimum was found by using the gradient and the updated hessian (B).

$$\underset{\sim}{H} = \underset{\sim}{B}^{-1} \tag{2.6}$$

$$E(x) = E_k + g_k^T (x-x_k) + \frac{1}{2}(x-x_k)^T B_k(x-x_k) \tag{2.7}$$

$$\frac{dE}{dx} = g(x) = g_k + B_k(x-x_k) = 0 \tag{2.9}$$

$$p_k = x-x_k = -B_k^{-1}g_k = -H_k g_k \tag{2.10}$$

If the gradient is smaller than a threshold, or change in the geometry is very small, than it is stopped.

5) Minimization is continued with $E(x_k + \alpha p_k)$ mostly α is equal to 1. That is $x_{k+1} = x_k + p_k$ k=k+1 by returning to the second step.

The rate of convergence depends on the initial geometry and estimation of hessian. The initial hessian can be chosen in several different ways;

1) Unit matrix; all the structural information about geometry is discarded.

16

2) Empirical guess; the diagonal elements of matrix is calculated related with bond length, bond angle, torsion etc. 3) The full second derivative matrix can be calculated analytically or numerically [34].

We have used the method of Davidon, Fletcher and Powell [35-37] which is an iterative steepest descent method for finding a local minimum of a function with several variables. It has a guaranteed convergence. This method requires the gradient vector. In this method, there are simplifications by which certain orthogonality conditions which are important to the rate of solution are preserved.

2.4. Semi Empirical Methods

The exact solution of Schrodinger equation is not possible for many electron systems. However there are approximate methods for small molecules whose accuracy may be comparable to experimental results for such as H_2, LiH etc. But as the system size increases, the problem becomes more difficult. Semi-empirical methods [38] rely on approximate functions and parameters to take place of the necessary integrals such that the results either mimic ab-initio calculations or experimental findings.

The complete electronic hamiltonian for a molecule in atomic units is,

$$H = -\frac{1}{2} \sum_i \nabla_i^2 - \sum_A \sum_i \frac{Z_A}{r_{Ai}} + \sum_i \sum_j \frac{1}{r_{ij}} + \sum_A \sum_B \frac{Z_A Z_B}{r_{AB}} \quad (2.11)$$

The first term is the kinetic energy of electrons, and the others are potential energy terms between nuclei and electrons .This Hamiltonian can be partitioned into two parts,

$$H = H_1 + H_2 + V \quad (2.12)$$

$$H_1 = -\frac{1}{2} \sum_i \nabla_i^2 - \sum_A \sum_i \frac{Z_A}{r_{Ai}} \quad \text{(one-electron Hamiltonian)} \quad (2.13)$$

$$H_2 = \sum_i \sum_j \frac{1}{r_{ij}} \quad \text{(two- electron Hamiltonian)} \quad (2.14)$$

and

$$V = \sum_A \sum_B \frac{Z_A Z_B}{r_{AB}} \quad \text{(nuclear repulsion)} \quad (2.15)$$

If the proper combination of Slater determinants are used as the 2n-electron wavefunction :

$$\Psi = \frac{1}{\sqrt{2n)!}} \begin{vmatrix} \Psi_1(1)\alpha(1) & \Psi_1(1)\beta(1) & \dots \Psi_n(1)\alpha(1) & \Psi_n(1)\beta(1) \\ \Psi_1(2)\alpha(2) & \Psi_1(2)\beta(2) & \dots \Psi_n(2)\alpha(2) & \Psi_n(2)\beta(2) \\ \cdot & \cdot & \cdot & \cdot \\ \cdot & \cdot & \cdot & \cdot \\ \cdot & \cdot & \cdot & \cdot \\ \Psi_1(2n)\alpha(2n) & \Psi_1(2n)\beta(2n) & \dots \Psi_n(2n)\alpha(2n) & \Psi_n(2n)\beta(2n) \end{vmatrix}$$

$$(2.16)$$

Then the expectation value of the energy is:

$$\langle E \rangle = \langle \Psi | H | \Psi \rangle + V \qquad (2.17)$$

$$\langle E \rangle = 2 \sum_i^n H_{ii} + \sum_{i,j}^n (2J_{ij} - K_{ij}) + V \qquad (2.18)$$

where H_{ii} is the core matrix element and J_{ij}, K_{ij} coulomb and exchange integrals respectively.

$$H_{ii} = \int \Psi_i(1) H_1(1) \Psi_i(1) d\tau_1 \qquad (2.19)$$

$$J_{ij} = \int \Psi_i(1) \Psi_i(1) \frac{1}{r_{12}} \Psi_j(2) \Psi_j(2) d\tau_1 d\tau_2 \qquad (2.20)$$

$$K_{ij} = \int \Psi_i(1) \Psi_j(1) \frac{1}{r_{12}} \Psi_i(2) \Psi_j(2) d\tau_1 d\tau_2 \qquad (2.21)$$

Introducing Lagrange multipliers for orthogonality conditions,

$$\langle G \rangle = \langle E \rangle - 2 \sum_{i,j} \varepsilon_{ij} S_{ij} \qquad (2.22)$$

and applying variational calculus we have the condition:

$$\delta G \equiv \delta \langle E \rangle = 0 \qquad (2.23)$$

When molecular orbitals are expanded as linear combinations of atomic orbitals (LCAO),

$$\Psi_i = \sum_p c_{ip} \phi_p \qquad (2.24)$$

Equation   2.23   becomes:

$$\sum_q (F_{pq} - E_i S_{pq}) c_{iq} = 0 \qquad (2.25)$$

with the Fock matrix element

$$F_{pq} = H_{pq} + \sum_{st} P_{st} \left[(pq|st) - \frac{1}{2} (ps|qt) \right] \qquad (2.26)$$

and the overlap integral

$$S_{pq} = \int \phi_p \phi_q \, d\tau \qquad (2.27)$$

In the above equations :

$$H_{pq} = \int \phi_p H \phi_q \qquad (2.28)$$

$$(pq|st) = \iint \phi_p(1) \phi_q(1) \frac{1}{r_{12}} \phi_s(2) \phi_t(2) \qquad (2.29)$$

where $P_{st} = 2 \sum_{j=1} c_{js} c_{jt}$ density matrix element.

The majority of semi-empirical methods are based on
the zero-differential overlap (ZDO) approximation. Although
there are many different parametrizations using ZDO, the
commonly used ones are MINDO/3 [15], MNDO [16] and AM1
[17]. In all of these methods almost all terms in energy
expression (Coulombic repulsion, electron-core attraction,
core-core repulsions, one-center exchange terms) are
evaluated by semi-empirical functions and these functions
contain numerical parameters that can be adjusted to fit

experimental data instead of analytical solutions of these integrals.

The last development of these methods is the AM1 (Austin Model 1) [17]. It is slightly different then MNDO, in that it modifies CRF (Core Repulsion Function) by adding gaussian terms. This is supposed to reduce excessive interatomic repulsion at large separations.

By using these approximate methods, quantum mechanical calculations for some very large molecules are possible with appropriate computer times.They are mostly used in the structural calculations of organic compounds.

RESULTS AND DISCUSSION

We tried to investigate a large number of high symmetry structures for 2 to 6 atom clusters. A complete list is given in figure 3. Even though this list is by no means complete, the energetically most favorable structures are included.

As the first step, bond lengths and certain angles are optimized with 2-body potential such that initial symmetries of clusters are preserved. The results are given in tables 1-3.

We observe that higher dimensional cases are more stable. For example three dimensional clusters are more stable than two and one-dimensional ones. It is well known that the linear structure is highly unstable when only 2-body potential is used. Since one of the aims is to study the effects of 3-body forces, we then added the scaled Axilrod-Teller potential. In figure 4-7 (a), the energies are plotted as functions of three body intensity parameter (Z^*) keeping previously optimized geometries. In figure 4-7 (b), the same functions are plotted by allowing each structure to be reoptimized under 3-body potential. In all optimized structures, the second derivative matrix Hessian is diagonalized and eigenvalues are analyzed. We did not find any negative eigenvalue showing that studied structures correspond to local or global minima.
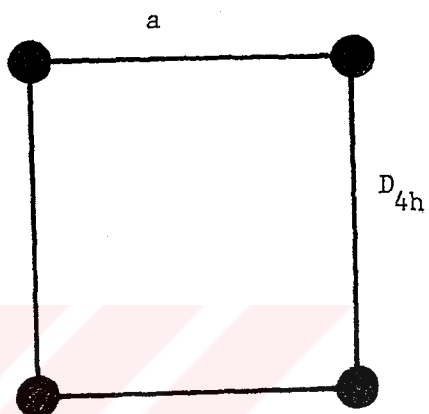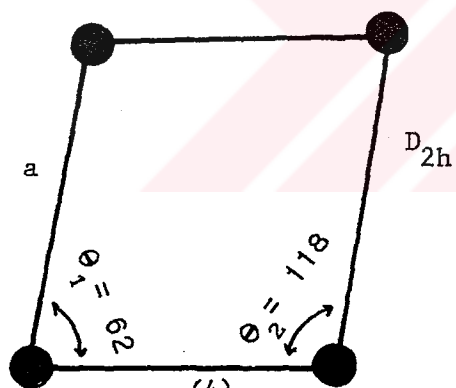
Figure 3.a. Clusters (2,3,4)
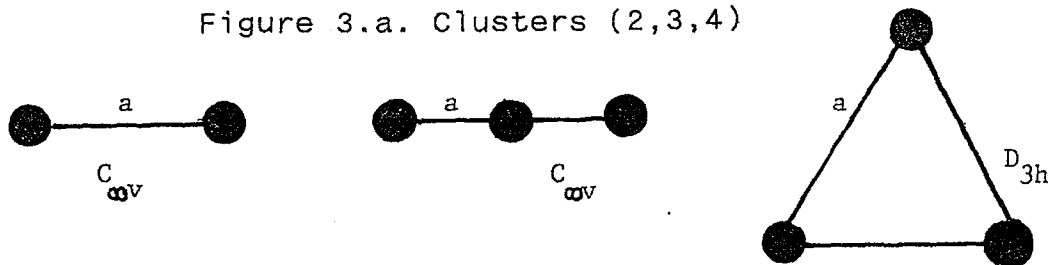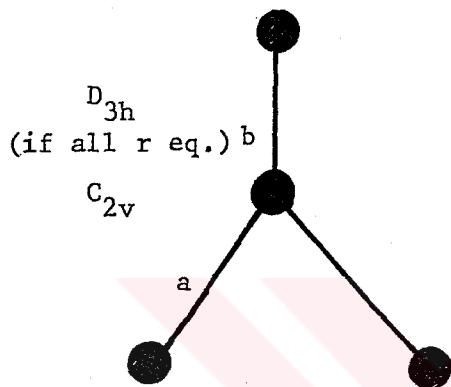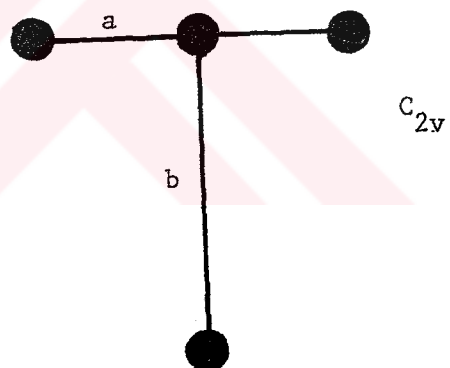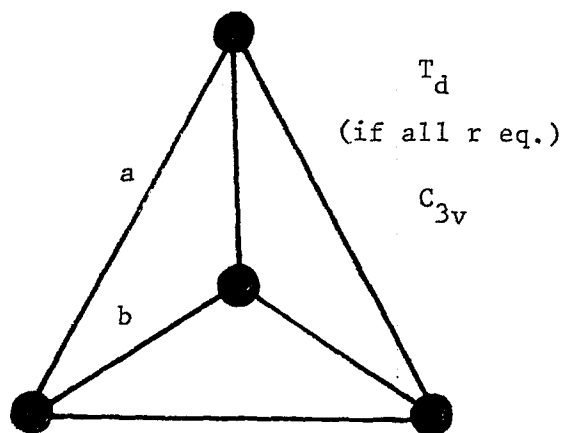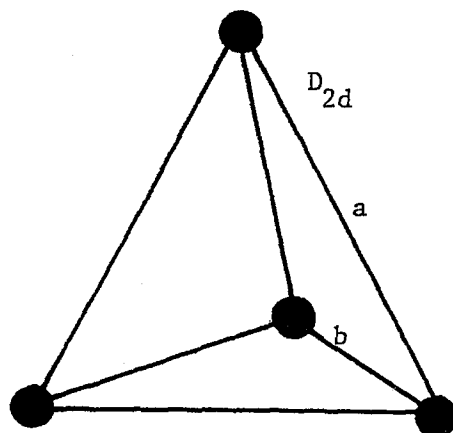
Figure 3.b. Clusters (5)
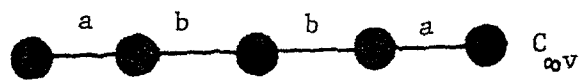
(1)
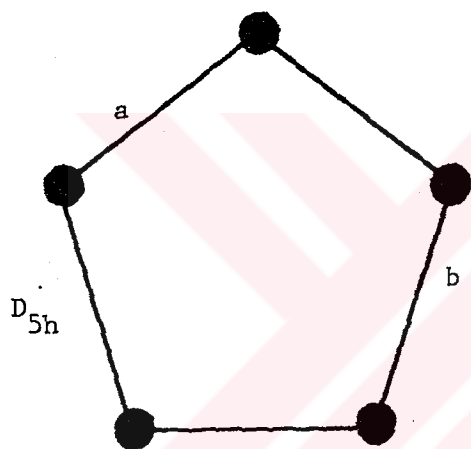
(2)
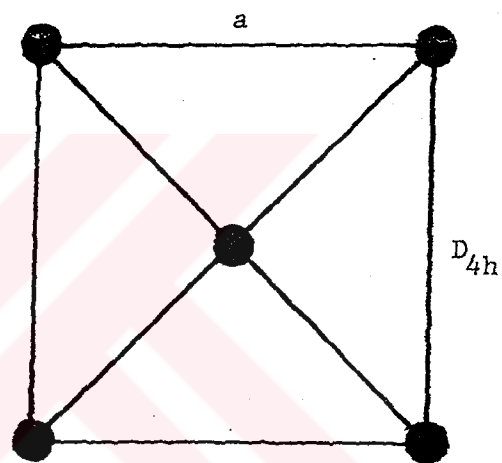
(3)
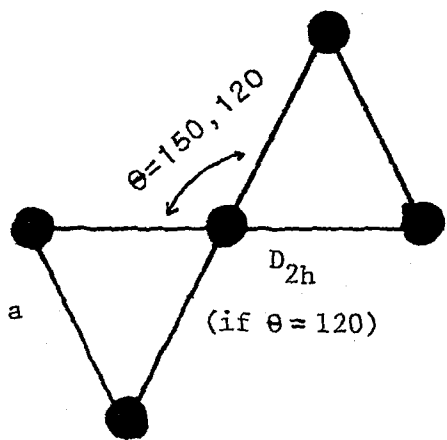
(7+4)
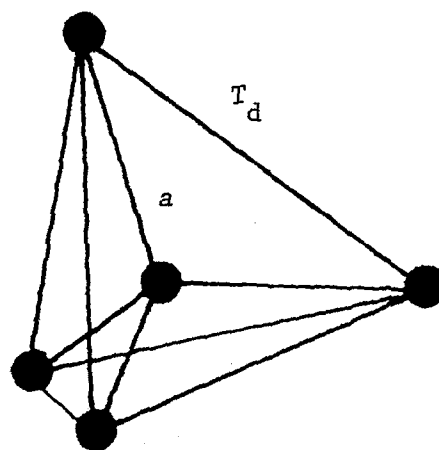
(5)

24

Figure 3.b. (Continued)
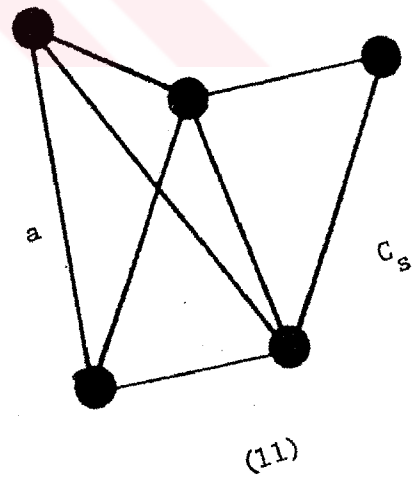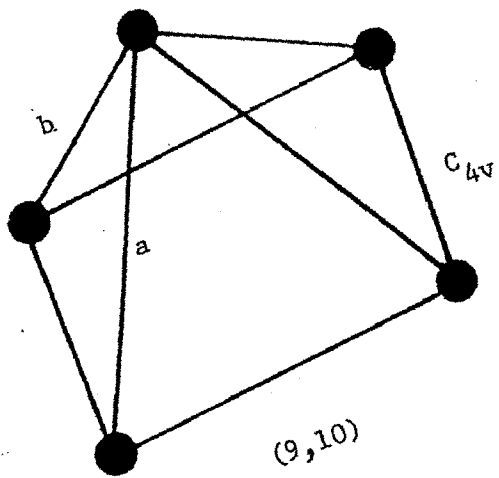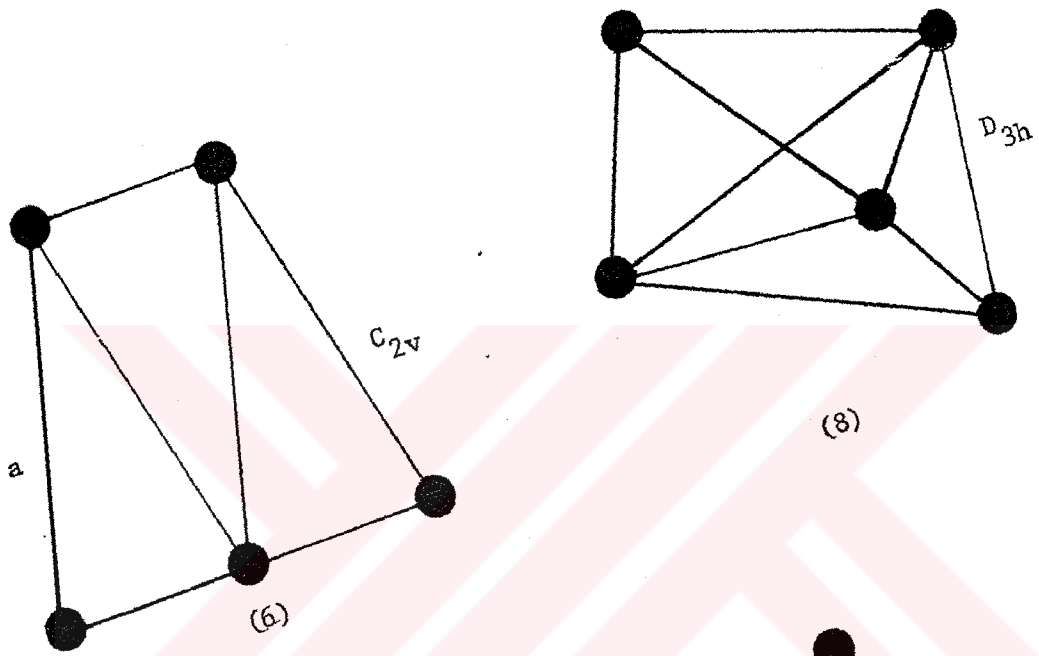
C_{2v}

a

(6)

D_{3h}

(8)

b

C_{4v}

a

(9,10)

a

C_s

(11)

25

Figure 3.c. Clusters (6)

Figure 3.c. (Continued)

a

C_{2h}

(7)

D_{5h}

a

(8)

a

b

C_{5v}

(9)

C_{4v}
(if all r eq.)

a

b

(10)

D_{3h}

c

b

a

(11)

D_{3h}

a

(12,13)

27

Figure 3.c. (Continued)

C_{4v}

C_{2h}

(15)

(14)

D_{2h}

C_{2v}

(17)

(16)

O_h

C_{2v}

(19)

(18)

28
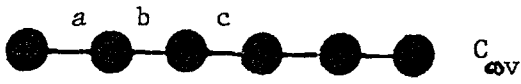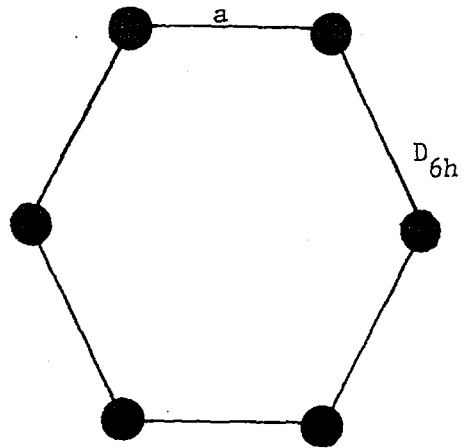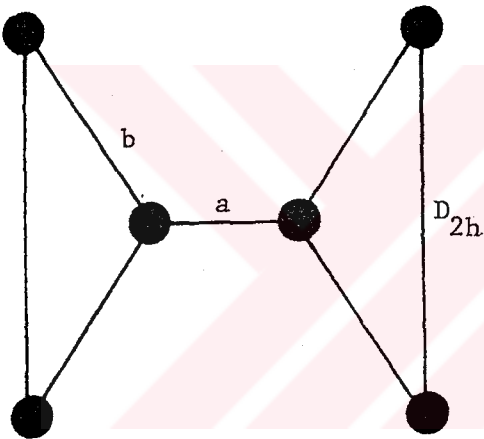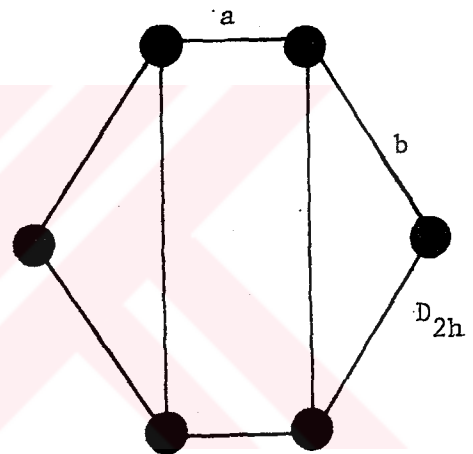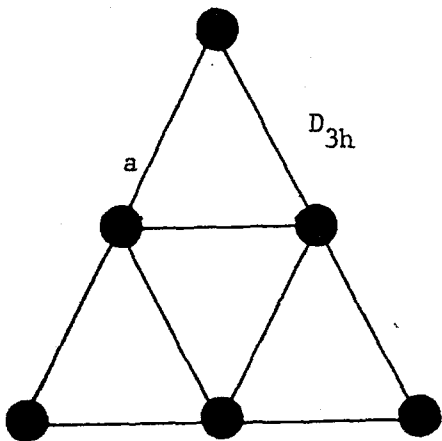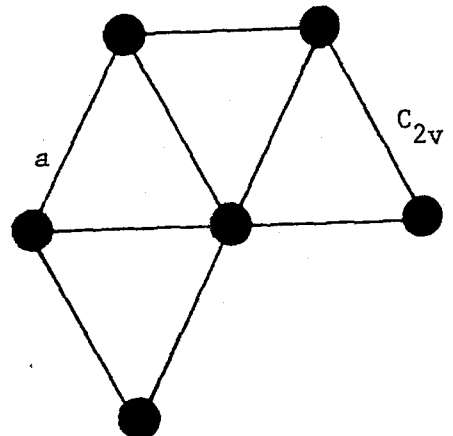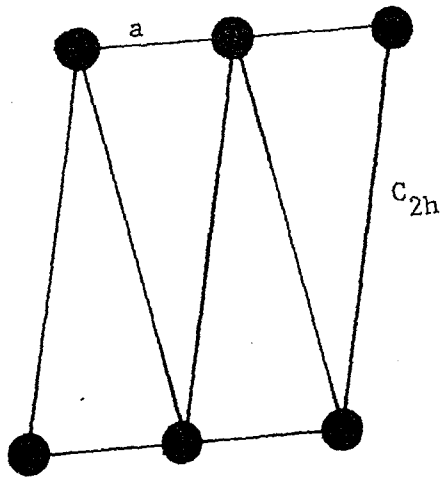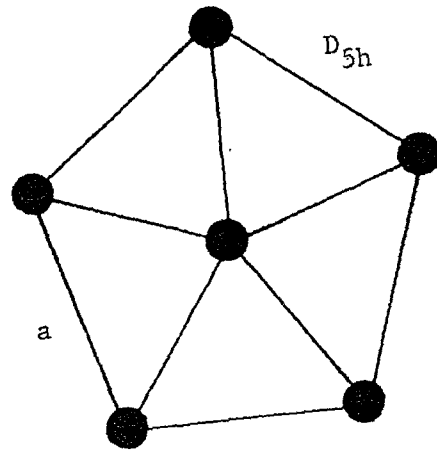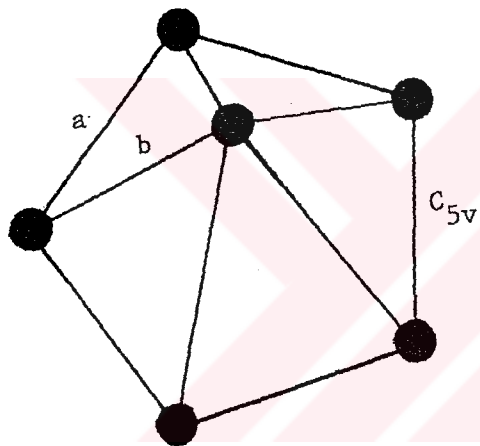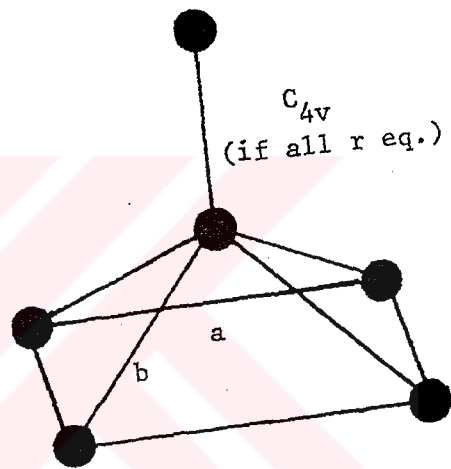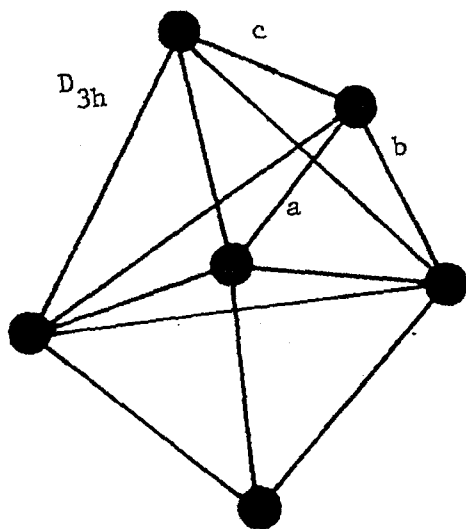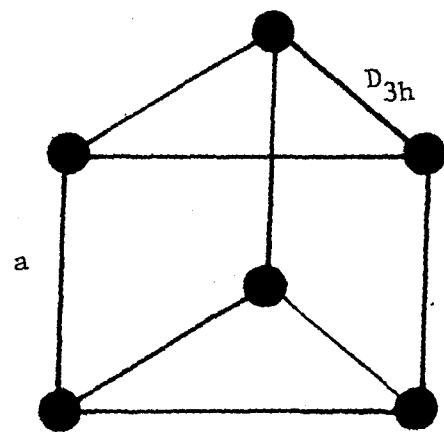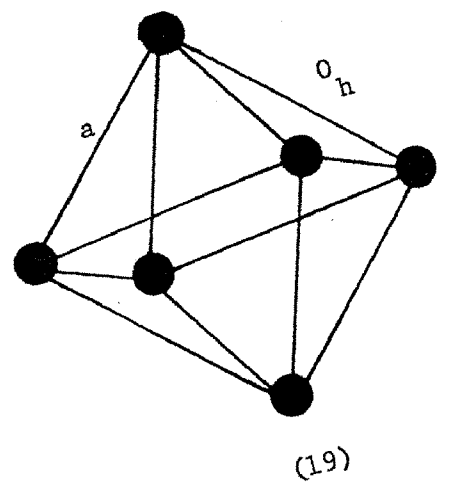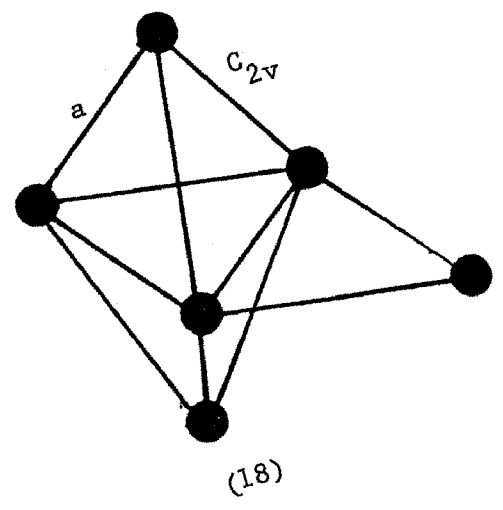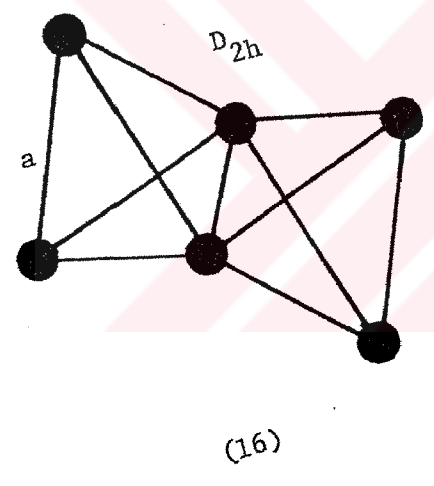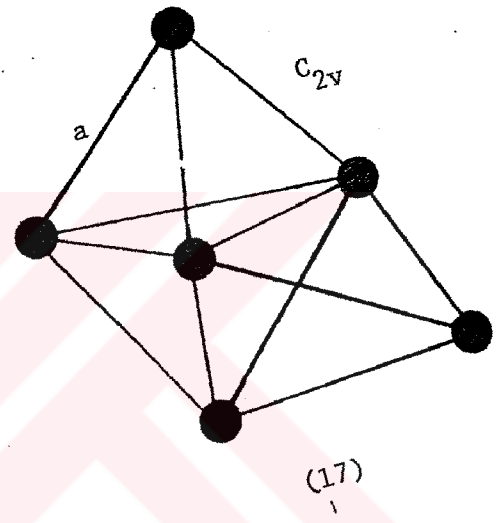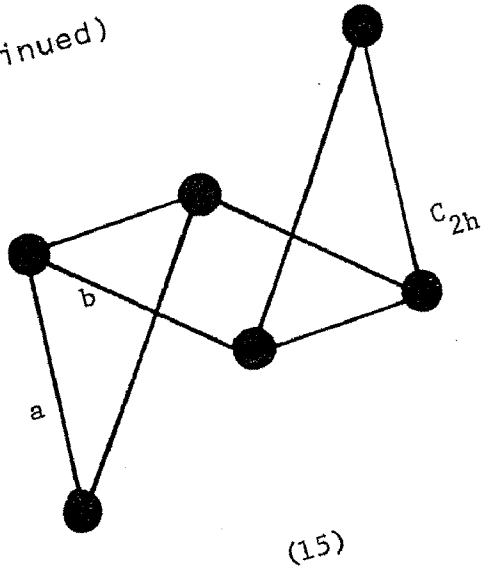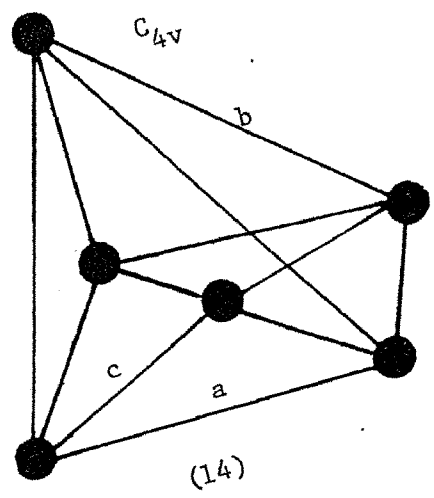
Table 1. Static Results for 2,3 and 4-Atom Clusters with Two Body
Potential Only.

NO	STRUCTURES	E	R(a)	R(b)	REMARKS
C2	LINEAR	-0.250	1.122	-	
C3	TRIANGLE	-0.750	1.122	-	
C3	LINEAR	-0.508	1.121	-	all r opt $\longrightarrow$ aa
6	PYRAMID	-1.500	1.122	-	
7	D.PYRAMID	-1.279	1.193	1.033	θ_d = 90.0 r,$\theta_d$op t $\longrightarrow$ rhom.
4	RHOMBUS	-1.268	1.120	-	
3	SQUARE	-1.120	1.113	-	rectangle$\longrightarrow$square
5	TSHAPE(aba)	-0.880	1.111	1.104	r's,$\theta_d$opt$\longrightarrow$ rhom.
2	PLANAR(aaa)	-0.805	1.116	-	r's,$\theta_d$opt$\longrightarrow$ rhom.
1	LINEAR(aba)	-0.766	1.121	1.120	all r opt$\longrightarrow$aba

Table 2. Static Results for 5-Atom Clusters with Two Body
Potential Only.

NO	STRUCTURES	E	R(a)	R(b)	REMARKS
8	TR.BIPYR	-2.276	1.124	1.120	
9	SQPYR2	-2.120	1.113	1.122	R(a) sq.,R(b) pyr.
10	SQPYR1	-2.119	1.117	-	all R's equal
11	DISTOR.SQPYR	-2.077	1.119	-	
6	W.3TRIANGLE(*)	-1.794	1.12	-	
7	BFLY2(*)	-1.588	1.117	-	θ=150 R's,θ opt→wtrian*
3	RECTANGLE	-1.553	1.929	1.125	R(c)=1.117 R's ,θ opt→θ=60.0
4	BFLY1(*)	-1.552	1.119	-	θ=120 R's,θ opt→wtrian*
2	PENTAGON	-1.389	1.113	-	
5	TETRAHEDRAL	-1.160	1.109	-	
1	LINEAR(aaaa)	-1.025	1.120	-	abab opt→aaaa
1	LINEAR(abba)	-1.025	1.121	1.119	R's opt→abba

30

Table 3. Static Results for 6-Atom Clusters with Two Body
Potential Only.

NO	STRUCTURES	E	R(a)	R(b)	REMARKS
19	OCTAHEDRAL	-3.178	0.790	-	
17	WITH.3PYRAMID	-3.075	1.120	-	
18	DIST.OCTAHEDRA	-2.913	1.117	-	
16	WITH.2PYR	-2.905	1.118	-	
9	PENT.PYR	-2.639	0.947	0.603	
12	BOAT CONF.1	-2.615	1.112	1.104	rectangular boat
13	BOAT CONF.2	-2.613	1.110	-	square boat
10	SQPYR2	-2.420	1.113	1.119	R(a)sq,R(b) pyr R(c)=1.11
15	CHAIR.CONF.	-2.377	1.112	1.096	
6	WITH.4TRIAN	-2.339	1.119	-	
5	WITH.TRIANGLE	-2.328	1.119	-	
7	ZIGZAG	-2.322	1.120		
4	DISTOR.HEXGON	-2.160	1.110	1.118	
8	PENTAGON	-2.142	1.276	-	
3	WITH.2TRIAN	-1.793	1.115	1.121	
14	SQPYR1	-1.775	1.094	1.088	
11	TR.BIPYR	-1.694	1.098	1.095	
2	HEXAGON	-1.635	1.115	-	
1	LINEAR(abcba)	-1.284	1.1209	1.1194	R(c)=1.1193 all r opt→abcba

a) Geometry for 2-Body reults
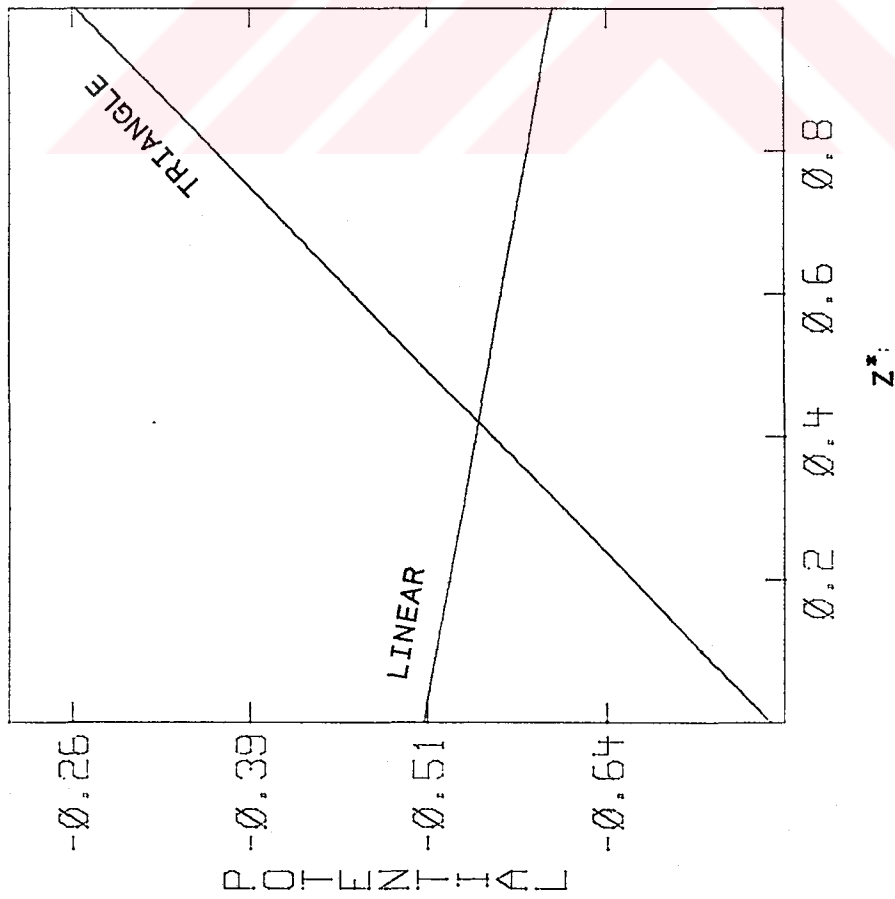
b) Optimized Geometry
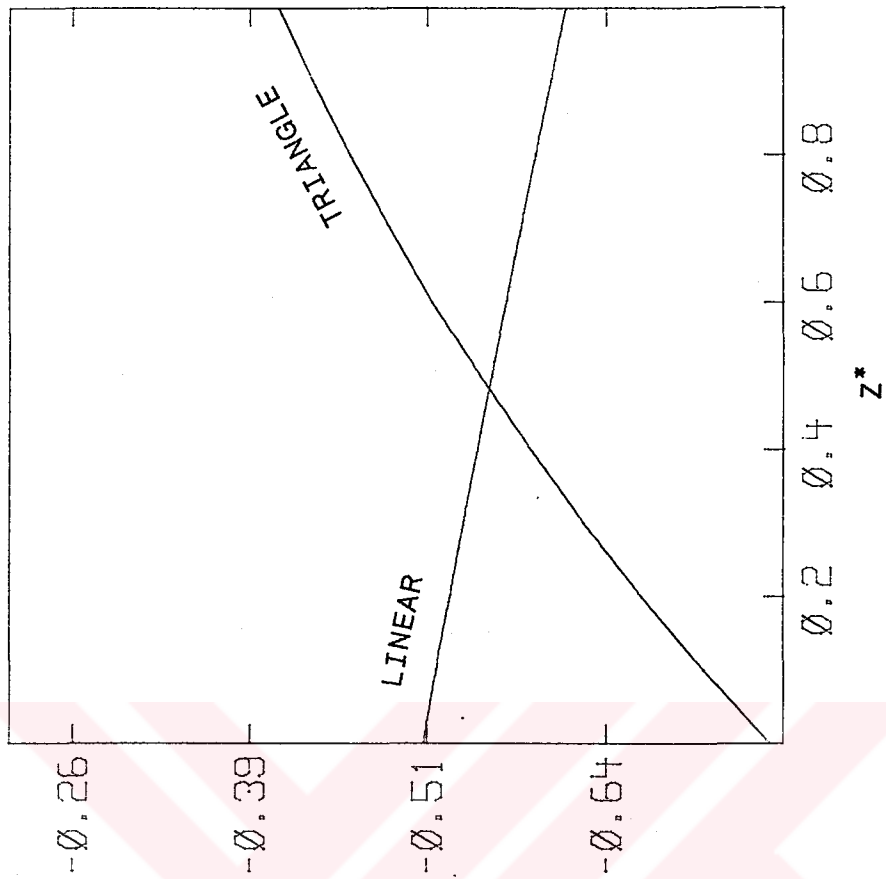
Figure 4. Total potential energy of 3 atoms as a function of z^*

32

a) Geometry for 2-Body results.

b) Optimized geometry.

Figure 5. Total potential energy of 4 atoms as a function of z*

Figure 6. Total potential energy of 5 atoms as a function of z^*

a) Geometry for 2-Body results.
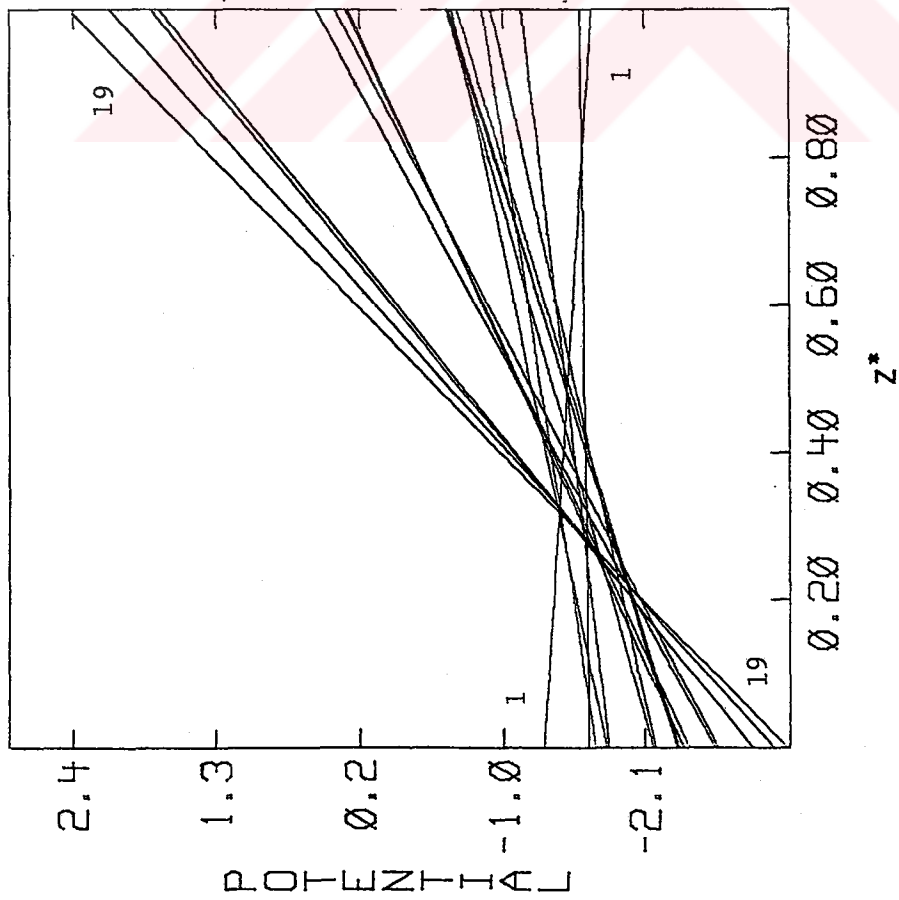
b) Optimized geometry.
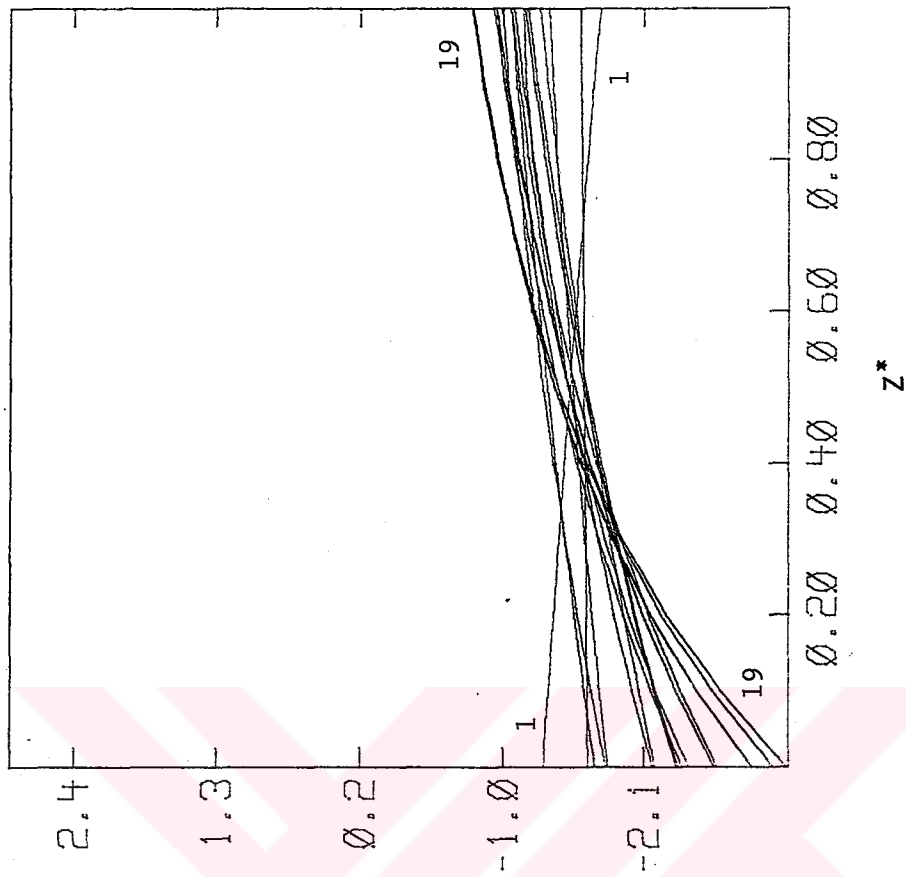
Figure 7. Total potential energy of 6 atoms as a function of z^*

35

In figure 4-7 (a), at large Z^* values the energy separation for different structures is larger in comparison to figure 4-7 (b). In the latter case the energies are closer. Also, in figure 4-7 (a) after $Z^* = 0.6$, there is not much change in the ordering, but in figure 4-7 (b), this threshold is around 0.9. For sufficiently large Z^* ,the ordering is almost same for frozen and optimum structures.

In all cases linear type of structure is the most stable one at Z^* larger than an average value of 0.6. At large Z^* one and two dimensional structures are more stable than three dimensional structures being just the opposite of two-body case. For Z^* larger than about 0.4, the most stable three dimensional conformation starts to lose its stability.
At Z^* in between 0.4-0.6 the energies of most of the structures are much more closer, compared to very small and very large Z^*. After 0.8 there are no more qualitative changes. The results at $Z^*= 0.8$ are given in tables 4-6 from the most stable structure to the least stable structure.

Finally we wanted to find out whether there is an optimum range for three-body-force-strength parameter such that these static calculations may be used to study a real cluster system. Using the AM1 method same structures are optimized for Carbon clusters and the results are given in table 7-9. We also made calculations with MINDO/3 and MNDO

Table 4. Static Results for 2,3,4-Atom Clusters at Z^*=0.8

NO	STRUCTURES	E	R(a)	R(b)	REMARKS
C2	LINEAR	–	–	–	
C3	LINEAR	−0.585	1.101		all r opt→aa
C3	TRIANGLE	−0.455	1.197		
1	LINEAR(aba)	−0.935	1.099	1.083	
2	PLANAR(aaa)	−0.824	1.113	–	R's opt→all r eq
3	SQUARE	−0.769	1.168	–	
4	RHOMBUS	−0.769	1.168	–	rhom → sq
5	TSHAPE(aba)	−0.751	1.116	1.165	
6	PYRAMID	−0.577	0.736	1.040	Z=1.0 pyr→planar
7	DPYRAMID	−0.560	1.330	1.152	

Table 5. Static Results for 5-Atom Clusters at Z^*=0.8

NO	STRUCTURES	E	R(a)	R(b)	REMARKS
1	LINEAR(abba)	−1.287	1.098	1.081	
1	LINEAR(aaaa)	−1.283	1.090	−	
2	PENTAGON	−1.165	1.138	−	
3	RECTANGLE	−1.026	2.004	1.206	
4	BFLY1	−1.023	1.181	−	θ=120
5	TETRAHEDRAL	−1.007	1.129	−	
6	W.3TRIANGLE	−0.997	1.209	−	
7	BFLY2	−0.995	1.187	−	θ=150
8	TR.BIPYR	−0.852	1.697	1.224	
9	SQPYR2	−0.820	1.199	1.407	
10	SQPYR1	−0.800	1.272	−	
11	DISTOR.SQPYR	−0.783	1.274	−	

Table 6. Static Results for 6-Atom Clusters at $Z^*=0.8$

NO	STRUCTURES	E	R(a)	R(b)	REMARKS
1	LINEAR(abcba)	−1.640	1.098	1.080	R(c) 1.078
2	HEXAGON	−1.587	1.119	−	
3	WITH.2TRIAN	−1.390	1.078	1.178	
4	DISTOR.HEXAGON	−1.384	1.133	1.203	
5	WITH.TRIANGLE	−1.321	1.205	−	
6	WITH.4TRIAN	−1.293	1.208	−	
7	ZIGZAG	−1.292	1.208	−	
8	PENTAGON	−1.201	1.375	−	
9	PENT.PYR	−1.191	0.980	1.195	
10	SQPYR2	−1.163	1.218	1.319	R(c)=1.101
11	TR.BIPYR	−1.125	1.152	1.161	
12	BOAT CONF.1	−1.091	1.279	1.197	
13	BOAT CONF.2	−1.077	1.247	−	
14	SQPYR1	−1.063	1.155	1.226	
15	CHAIR.CONF.	−1.042	1.246	1.207	
16	WITH.2PYR	−0.923	1.303	−	
17	WITH.3PYRAMID	−0.921	1.318	−	
18	DIST.OCTAHEDRA	−0.913	1.306	−	
19	OCTAHEDRAL	−0.907	0.936	−	

Table 7. AM1 Results for 2,3,4-Atom Clusters

NO	STRUCTURES	E (eV)	R(a)	R(b)	REMARKS
C2	LINEAR	−247.08	1.164	−	
C3	LINEAR	−375.47	1.288	−	All r opt→ aa
C3	EQ.TRIANGL	−370.05	1.415	−	r's,θ opt→linear r's opt→nonsymmet. trian. θ' 50,60,70
1	LINEAR.aba	−500.77	1.309	1.279	abc opt→aba
	DPYRAMID *	−497.07	1.459	1.487	$\theta_d$opt →180
4	RHOMBUS *	−497.08	1.464	−	opt θ_1=118 θ_2=62
5	T-SHAPE(ab)	−496.65	1.350	1.483	abc opt→aba
3	SQUARE	−495.60	1.449	−	
2	PLANAR.aaa	−494.83	1.393	−	
6	PYRAMID	−488.44 −490.88	1.560 1.82	− 1.48	all r equal R(a)→base triangle R(b)→pyr.
7	DPYRAMID	−490.21	1.629	−	θ = 60.0

Table 8. AM1 Results for 5-Atom Clusters

NO	STRUCTURES	E (eV)	R(a)	R(b)	REMARKS
1	LINEAR(abba)	−629.42	1.280	1.278	abcd opt→abba
1	LINEAR(aaaa)	−629.42	1.279	−	abab opt→aaaa
3	RECTANGLE	−620.57	2.568	1.487	R(c)=1.484 R's,θ opt→θ=60.0
6	W.3TRIANGLE	−620.54	1.478	−	
2	PENTAGON	−619.33	1.356	−	
8	TR.BIPYR	−619.31	2.282	1.540	
7	B.FLY2	−619.24	1.452	−	θ = 150
4	B.FLY1	−619.16	1.444	−	θ = 120
9	SQPYR2	−615.95	1.486	1.755	R(a) sq,R(b) pyr
5	TETRAHEDRAL	−615.26	1.450	−	
11	DISTOR.SQPYR	−615.21	1.557	−	
10	SQPYR1	−615.16	1.569	−	all R equal
8	TR.BIPYR	−612.69	1.564	−	all R equal

41

Table 9. AM1 Results for 6-Atom Clusters

NO	STRUCTURES	E (eV)	R(a)	R(b)	REMARKS
1	LINEAR(abcba)	−755.20	1.294	1.276	abcde opt→abcba R(c)=1.278
2	HEXAGON	−751.70	1.317	—	
3	WITH.2TRIAN	−748.33	1.321	1.434	
4	DISTOR.HEXAGON	−747.32	1.356	1.499	
7	ZIGZAG	−745.46	1.484	—	
6	WITH.4TRIAN	−743.52	1.481	—	
5	WITH.TRIANGLE	−743.12	1.467	—	
12	BOAT CONF.1	−741.25	1.552	1.503	rectangular boat
13	BOAT CONF.2	−741.15	1.545	—	square boat
9	PENT.PYR	−740.78	1.464	2.050	
15	CHAIR CONF.	−740.66	1.569	1.528	
18	DIST.OCTAHEDRA	−740.28	1.608	—	
10	SQPYR2	−739.53	1.558	1.691	R(a) sq,R(b) pyr R(c)=1.305
17	WITH.3PYRAMID	−739.28	1.609	—	
16	WITH.2PYR	−737.80	1.611	1.386	
14	SQPYR1	−736.25	2.098	2.190	R(c)=1.483 a,c(sq) R(d)=1.611 d(pyr)
11	TR.BIPYR	−735.78	1.484	2.570	R(c)=2.132 R(a,b)trian;R(c)py
8	PENTAGON	−735.28	1.455	—	
19	OCTAHEDRAL	−733.23	1.673	—	Ra(sq) Rb(pyr)opt → all r equal

method. Since their orders are approximately same only those from AM1 are displayed. In all cases the optimum geometry of the lowest energy structures are linear. These results are in good agreement with ab-initio [39-50,54] studies and some experimental data [51,52,53]. Again, linear conformation is preferred energetically to two dimensional clusters which were in turn more stable than three dimensional clusters. The comparison with other results are given in table 10. All studies indicate that, the ground state structure of C_3 and C_5 is linear. For C_4 and C_6 there are some discrepancies. [40,42, 46, 49]. According to Ritchie [40], Rao [42], and Raghavachari [46] the favorite structure of C_4 is rhombus having a little energy difference (about 0.3 eV) with the linear one. But ESR results of Graham [51] shows that the linear conformation is the lowest energy state. And also according to Raghavachari [46], the stable structure of C_6 is distorted hexagon instead of linear.

We see that the two-body potentials do not provide a good description of the Carbon clusters. Even for small Z^* values, this qualitatively incorrect ordering of stability prevails. Only when Z^* reaches the value of 0.8 then there is a good similarity between classical and quantum mechanical results.

Table 10. For Carbon Clusters, Comparison of AM1 Results (Bond
Lengths and Ground Configuration) with Other Results.
The Bond Lengths belong to Linear Configuration if not
Specified.

C_2 C_3 C_4 C_5

$C \overset{a}{—} C$; $C \overset{a}{—} C \overset{a}{—} C$; $C \overset{a}{—} C \overset{b}{—} C \overset{a}{—} C$; $C \overset{a}{—} C \overset{b}{—} C \overset{b}{—} C \overset{a}{—} C$;

C_6

$C \overset{a}{—} C \overset{b}{—} C \overset{c}{—} C \overset{b}{—} C \overset{a}{—} C$
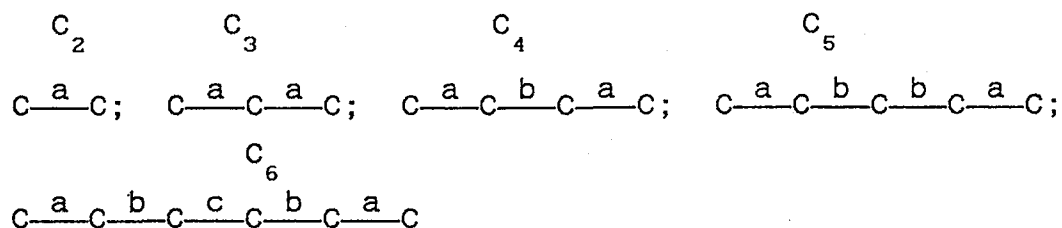
METHOD	C_2	C_3	C_4	C_5	C_6
AM1	1.164(a)	1.288(a)	1.309(a) 1.279(b)	1.280(a) 1.278(b)	1.293(a) 1.275(b) 1.269(c)
SDHF/DZP [39]	1.260	1.290	1.310 1.280	1.290 1.280	–
SCF-UHF [42]	1.350	1.300	Rhombus 1.260 –	–	–
HF/6-31G* [46]	1.245	1.278	Rhombus 1.425 $\theta=61.5$	–	–
RHF/DZP [47]	1.260	1.290	1.310 1.280	1.290 1.280	1.300 1.280 1.280
SRCI/3-21G* [40]	1.203	–	Rhombus 1.448(a) 1.500(b)	–	–
Experimental [52]	1.240	–	–	–	–
MBPT/CC-TZP [45]	–	1.2997	–	1.2967 1.2862	–
Experimental [53]	–	1.277	–	–	1.293

Table 10.(Continued)

METHOD	C_2	C_3	C_4	C_5	C_6
ESR+HF/DZ [41]	–	–	1.306 1.282	–	1.299 1.280 1.273
HF /6-31G* [50]	–	–	1.300 1.276	–	–
SCF CEPA-1 [43]	–	–		1.289 1.283	–
MP2/6-31G* [44]	–	–	–	1.300 1.291	–
MCSCF,MRCI [48]	–	–	–	–	1.298 1.280 1.265
HF/6-31G* [49]	–	–	–	–	distort. hexagon $\theta=90.4$ 1.316

Some of the Abbreviations in Above Table

SHF/DZP   Single Determinant Hartree-Fock level using Double Zeta

plus Polarization basis set.

SCF-UHF   Self Consistent Field, Unrestricted Hartree-Fock.

HF/6-31G*   Hartree-fock level calculation using 6-31G basis set.

RHF   Restricted Hartree-Fock

SRCI/3-21G* Single Reference Configuration Interaction.

MBPT/CC-TZP Many Body Perturbation Theory using Coupled Cluster

theory with triple zeta plus polarization basis set.

ESR   Electron Spin Resonance.

CEPA   Couple Electron Pair Approximation

MCSCF   Multi configuration SCF

MRCI   Multi referance Configuration Interaction.

If we compare the structures and the ordering for classical ($Z^*=0.8$) and quantum mechanical results:

a) C_3 The linear form is more stable than the triangular form in both sets of calculations.

b) C_4 7 structures are studied. The linear one is the energetically most stable structure and distorted pyramid is the least stable structure in both methods. The ordering is given in table 11. The main difference in this case is the planar(2) structure. The classical calculations overemphasize the stability of this cluster as expected since this geometry allows the maximum three-body attraction. In the case of trigonal pyramidal conformation, at $Z^*=1.0$ there is an abrupt change in the structure during the optimization. It goes to planar conformation suddenly. The same case observed in the AM1 result. The distance between the fourth atom to the center of the base-triangle becomes shortened. This forces the three dimensional structure to the planar structure.

c) C_5 The number of structures studied is 11. The ordering is given in table 12. If we use AM1 results as the correct stability criterion, then we see a very good match of results. The linear ones are the most stable cases in both methods. The remaining geometries can be classified into two groups. There are basically two discrepancies in this grouping. Tetrahedral structure is again too stable due to

Table 11. Comparison of Quantum Mechanical Results with Static
Results for 4-Atom Clusters. Structure Numbers are
Written from the Most Stable to the Least Stable One.

AM1	$Z^*=0.8$	2-body
1	1	6
4	2	7
5	3	4
3	4	3
2	5	5
6	6	2
7	7	1

Table 12. Comparison of Quantum Mechanical Results with Static
Results for 5-Atom Clusters. Structure Numbers are
Written from the Most Stable to the Least Stable One.

AM1	$Z^*=0.8$	2-body
1	1	8
2	3	9
3	6	10
4	2	11
5	8	6
6	7	7
7	4	3
8	9	4
9	5	2
10	11	5
11	10	1

47

its unique shape offering large three-body attraction. The trigonal bipyramidal one is found to be less stable in contrast to the AM1 findings.

d) C_6 In this case there are 19 structures have been studied. The ordering is given in table 13. The order of the first seven structures are almost same, again linear being the most stable one and hexagonal the second stable structure. Also the octahedral is the least stable structure for both methods. Following the trends of the smaller clusters, pentagonal and trigonal bipyramidal clusters are too stable in classical calculations. Both boat and chair conformations as well as the distorted octahedral structures are found to be less stable than AM1 results. However the last one may be due to the difficult optimization of one of the dihedral angles as the structure tends to collapse into a planar shape upon optimization.

Overall in all 39 structures, we observe a fairly good qualitative fit of AM1 and classical results when three-body potentials with a relatively large intensity parameter are used. These results are displayed in figure 8.

We calculated an R value by taking the ratio of AM1 optimized distances to those from static calculations Standard deviations (σ) are calculated for each Z^* value. In figure 9, σ is plotted as a function of Z^*. Almost for all

Table 13. Comparison of Quantum Mechanical Results with Static Results for 6-Atom Clusters. Structure Numbers are Written from the Most Stable to the Least Stable One.

AM1	$Z^*=0.8$	2-body
1	1	19
2	2	17
3	3	18
4	4	16
5	7	9
6	6	12
7	5	4
8	12	10
9	13	15
10	9	6
11	15	5
12	18	7
13	10	4
14	17	8
15	16	3
16	14	14
17	11	11
18	8	2
19	19	1
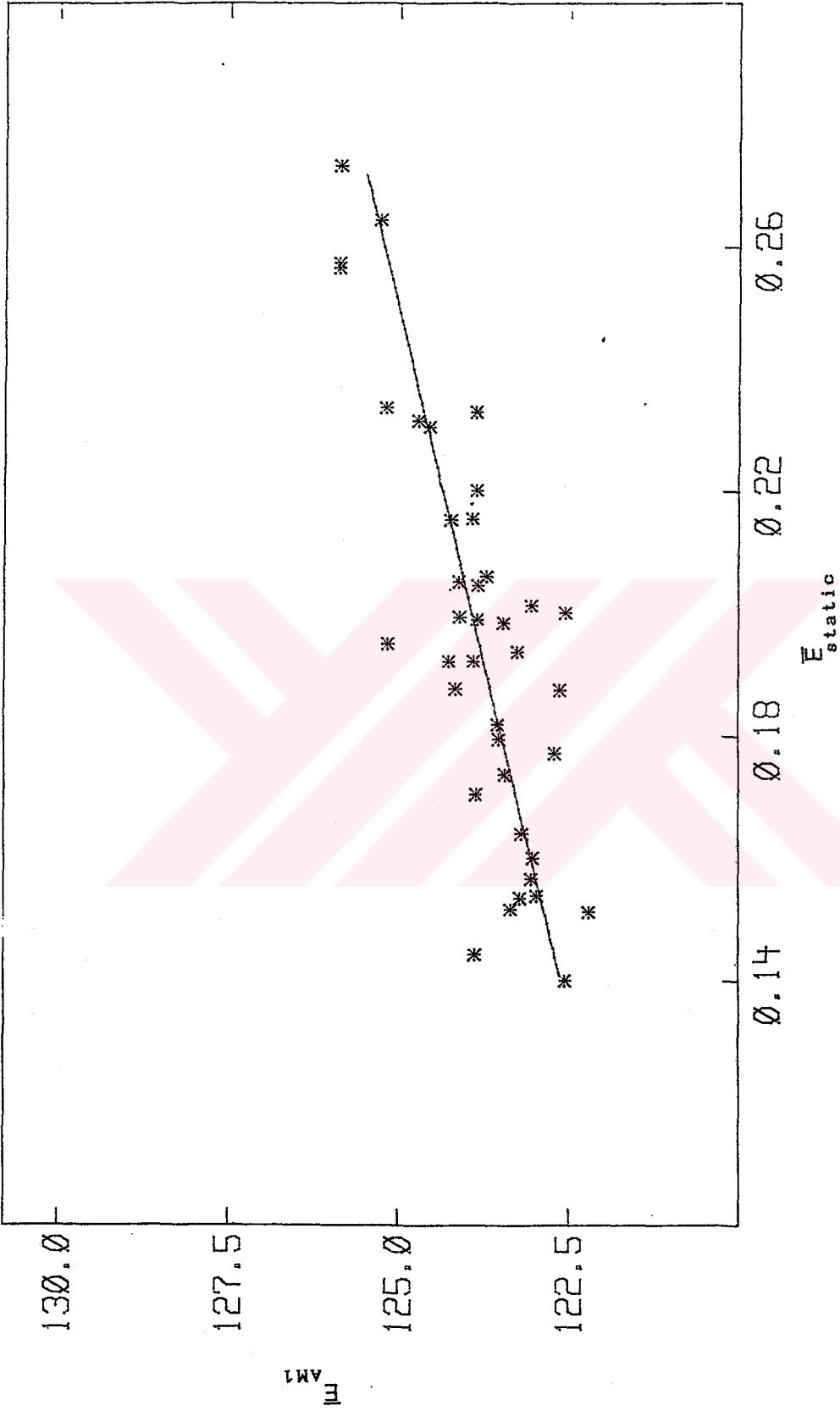
Figure 8. Correlation between classical and quantum mechanical energies per particle.

50
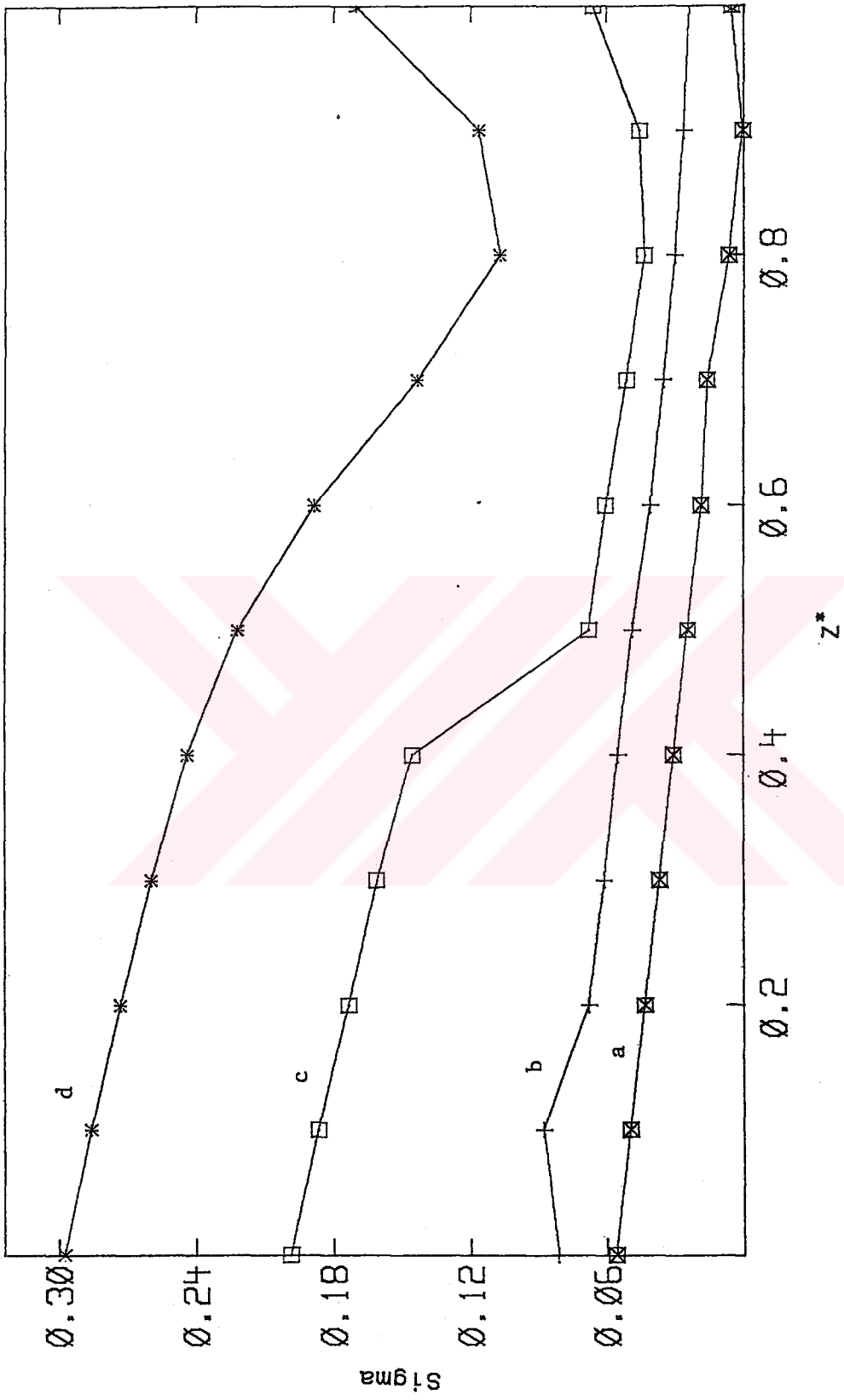
Figure 9. Standard deviation of $\dfrac{r_{AM1}}{r_{static}}$ as a function of Z for various size clusters (a:3, b:4, c:5, d:6)

size clusters, there is a minimum, around $Z^*=0.8$.

Finally the total three-body contributions are computed by comparison of three different energy calculations. Contribution to energy are obtained by subtracting the energy of two-body case from the $Z^*=0.8$ at nonoptimized geometries. The contribution due to the relaxation of the geometry is the difference between the optimum and nonoptimized structures. The ratio of 3-body potential versus 2-body potential in the case of optimum structures is given in tables 14-16.

Table 14. Three-Body Contribution in 4-Atom Clusters

No	energy contribution	geometry relaxation	total contribution	$\dfrac{E_{AT}}{E_{LJ}}$
1	-0.141	-0.028	-0.169	0.252
2	-0.019	0.000	-0.019	-0.119
3	0.433	-0.082	0.351	-0.269
4	0.771	-0.272	0.499	-0.267
5	0.153	-0.024	0.129	-0.139
6	1.444	-0.521	0.923	-0.460
7	1.131	-0.412	0.719	-0.433

Table 15. Three-Body Contribution in 5-Atom Clusters

No	energy contribution	geometry relaxation	total contribution	$\dfrac{E_{AT}}{E_{LJ}}$
1	-0.228	-0.034	-0.262	0.301
2	0.247	-0.023	0.224	-0.148
3	0.666	-0.139	0.527	-0.284
4	0.667	-0.138	0.529	-0.288
5	0.165	-0.013	0.152	-0.124
6	1.102	-0.305	0.797	-0.359
7	0.768	-0.175	0.593	-0.312
8	2.208	-0.983	1.225	-0.416
9	2.245	-0.927	1.318	-0.469
10	2.241	-0.946	1.295	-0.418
11	2.208	-0.914	1.294	-0.469

Table 16. Three-Body Contribution in 6-Atom Clusters

No	energy contribution	geometry relaxation	total contribution	$\dfrac{E_{AT}}{E_{LJ}}$
1	-0.307	-0.049	-0.356	-0.503
2	0.049	-0.001	0.049	-0.029
3	0.552	-0.149	0.403	-0.170
4	1.036	-0.259	0.776	-0.288
5	1.379	-0.371	1.008	-0.352
6	1.451	-0.405	1.046	-0.361
7	1.425	-0.394	1.030	-0.359
8	1.296	-0.355	0.941	-0.356
9	2.394	-0.946	1.448	-0.290
10	2.151	-0.893	1.258	-0.359
11	0.715	-0.146	0.569	-0.281
12	2.497	-0.961	1.536	-0.449
13	2.492	-0.968	1.524	-0.434
14	0.967	-0.255	0.711	-0.318
15	2.104	-0.768	1.336	-0.430
16	3.702	-1.720	1.983	-0.503
17	4.150	-1.996	2.154	-0.513
18	3.762	-1.762	2.000	-0.505
19	4.489	-2.218	2.271	-0.517

CONCLUSIONS

In this study the high-symmetry structures of Lennard-Jones clusters between 3 and 6 particles are analyzed. Geometrical parameters are optimized to minimize the energy using both two- and three-body forces of various strength. Similarly same structures are also optimized by the quantum mechanical AM1 method for Carbon clusters. Upon comparison of the stability orders with respect to classical and quantum mechanical methods, it is seen that two-body forces represent the total interactions of the system rather poorly. For an optimum three-body strength parameter Z^* we have observed a strong similarity for the stability orders of both methods. We conclude that using pairwise potentials with nonadditive three-body terms, one can obtain at least qualitatively correct information about microcluster formation and stability. Since these calculations are much more economical compared to accurate ab-initio quantum calculations, it is conjectured that structural calculations of large size clusters would be feasible. The possible applications are Monte Carlo and Molecular Dynamics simulation studies of these and larger clusters with the parameters obtained from this study to find out about the total potential energy hypersurface and dynamical properties of clusters.

REFERENCES

1. Hoare, M.R., Advances in Chemical Physics, Vol.40 PP.49-135, (1979).

2. Halıcıoğlu, T., Bauschlicher Jr., C.W., Physics of Microclusters, Rep.Prog.Phys., Vol.51, PP.883-921, (1988).

3. Polymoropoulos, E.E, Brickmann, J. , Ber.Bungenges.Phys. Chem., Vol.87, PP.1190-1195, (1983).

4. Koutecky, J., Fantucci, P., Chem.Rev. , Vol.86, PP.539-587, 1986.

5. Brown, W.L., Freeman, R.R, Raghavachari, K., Schluter, M., Science, Vol.235, PP.860-865, 1987.

6. Phillips, J.C., Chem.Rev., Vol.86, PP.619-634, 1986.

7. Baird, N.Colin, J.Computational Chemistry, Vol.5, No.1, PP.35-43, 1984.

8. Hohl, D., Jones, R.O., J.Chem.Phys., Vol.89(11), PP.6823-6833, 1988.

9. Rao, B.K., Jena, P., Shillady, D.D., Physical Rewiew B, Vol.30, Number 12, PP.7293-7296, 1984

10. Xie, J., Northby, J.A., Freeman, D., Doll, J.D., J.Chem.Phys., Vol.91(1), PP.612-619, 1989.

11. Wales, J.D., J.Chem.Phys., Vol.91(11), PP.7002-7010, 1989.

12. Raghavachari, K., J.Chem.Phys., Vol.84(10), PP.5672-5686, 1986.

13. Feuston, B.P., Kalia, R.K., Vashishta, P., Physical Review B, Vol.35, PP.6222-6239, 1987.

14. Rohlfing, C.M., Raghavachari, K., Chem.Phys.Letters, Vol.167,Number 6, PP.559-565, 1990.

15. Bingham, R.C., Dewar, M.J.S., Lo, D.H., J.American Chem.Society, Vol.97, Number 6, PP.1285-1293, 1975.

16. Dewar, M.J.S., Thiel, W., J.American Chem.Society, Vol.99(15), PP.4899-4906, 1977.

17. Dewar, M.J.S., Zoebisch, E.G., Healy, E.F., J.American Chem.Society, Vol.107, PP.3902-3909, 1985.

18. Hoare, M.R., Pal, P., Advances in Physi cs, Vol.20, PP.161-196, 1971.

19. Polymoropoulos, E.E, Brickmann, J., Chem.Phys. Letters, Vol.96, Number 3, PP.273-275, 1983.

20. Halıcıoğlu, T., White, J.P., J. Vac.Sci.Technol., V.17(5), PP.1213-1215, 1980.

21. Halıcıoğlu, T., Takai, T.,Tiller, W.A., Surface Science, V.156, PP.556-562, 1985.

22. Halıcıoğlu, T., Pamuk, H.Ö., Surface Science, Vol.215, PP.272-280, 1989.

23. Halıcıoğlu, T., Petterson, G.M.L., Bauschlicher, C.W.,J.Chem.Phys., Vol.87(4), PP.2205-2213, 1987.

24. Halıcıoğlu, T., White, J.P., Surface Science, Vol.106, PP.45-50, 1981.

25. Halıcıoğlu, T., Phys.Stat.Sol.(b), Vol.99, PP.347. 1980.

26. Öksüz, İ., Surface Science, V.122, PP.L585-L592, 1982.

27. Blaisten-Brojas, E., Andersen, H.C., Surface Science, Vol.156, PP.548-555, 1985

28. Polymoropoulos, E.E, Brickmann, J., Chem.Phys. Letters, V.92, Number.1, PP.59-63, 1982

29. O. Hirschfelder, J.O., Curtiss, C.F., Bird, B.R., Molecular Theory of Gases and Liquids, PP.22-34, John Wiley and Sons, Inc., 1954.

30. Tildesly D.J., Allen, M.P., Computer Simulation of Liquids, Oxford Science Publications, Ch.1, 1989

31. Axilrod, B.M.,Teller, E., J.Chem.Phys., Vol.11, Number 6, PP.299-300, 1943.

32. Axilrod, B.M., J.Chem.Phys., Vol.17, PP.1349, 1949.

33. Axilrod, B.M., J.Chem.Phys., Vol.19, Number 6, PP.719-729, 1951.

34. Schlegel, B.H., Ab-Initio Methods in Quantum Chemistry-I, John Wiley and Sons. Ltd., PP.249-285, 1987.

35. Fletcher, R., Powell, M.J.D., Computer Journal, Vol.6., PP.163-, 1963.

36. Powell, M.J.D., Comp.J., Vol.7, PP.155-, 1964.

37. Fletcher, R., Reeves, C.M., Comp.J., Vol.7, PP.149-, 1964.

38. Pople, J.A, Beveridge, D.L., Approximate Molecular Orbital Theory, McGraw-Hill, New York, 1970.

39. Ewing, D.W., Pfeiffer, G.V, Chem.Phys.Letters Vol.86(4), PP.365-368, 1982.

40. Ritchie, J.P., King, H.F., Young, W.S., J.Chem.Phys., Vol.85(9), PP.5175-5182, 1986.

41. Zee, R.J.V., Ferrante, R.F., Zeringue, K.J., Weltner, W, Ewing, Jr D.W., J.Chem.Phys., Vol.88(6), PP.3465-3474, 1988.

42. Rao, B.K., Khanna, S.N., Jena, P., Solid State Communications, Vol.58, No.1, PP.53-56, 1986.

43. Botshwina, P., Sebald, P., Chem.Phys.Letters, Vol.165, Number 5,6, PP.485-493, 1989.

44. Martin, J.M.L., François, J.P., Gijbels, R., J.Chem.Phys. Vol.90(6), 1989.

45. Adamowicz, L., Kurtz, J., Chem.Phys.Letters, Vol.162, Number 4,5, PP.342-347, 1989.

46. Raghavachari, K., Binkley, J.S., J.Chem.Phys. Vol.87(4), PP.2191-2197, 1987.

47. Fan, Q., Pfeiffer, G.V., Chem.Phys.Letters, Vol.162, No.6, PP.472-478,1989.

48. Parasuk, V., Almlöf, J., J.Chem.Phys., Vol.91(2), PP.1137-1141, 1989.

49. Raghavachari, K., Whiteside, R.A., Pople, J.A, Pople, J.Chem.Phys. Vol.85(11), PP.6623-6628, 1986.

50. Whiteside, A. R., Raghavachari, K., Defrees, D.J., Pople, J.A, Schleyer,P.V.R., Chem.Phys.Letters, Vol.78, No.3, PP.538-540, 1981.

51. Graham, W.R.M., Dismuke, K.I., Weltner Jr., W., Astrophysical Journal, Vol.204, PP.301-310, 1976.

52. Rosen, B., Spectroscopic Data Relative to Diatomic Molecules, P.81, Pergaman, New York, 1970.

53. Gausset, L., Hertzberg, G., Lagerguïst, A., Rosen, B., Discussions Faraday Soc., Vol.35, PP.113-, 1963.

54. Pitzer, K.S., Clementi, E., J.American Chem.Soc., Vol.81, PP.4477, 1959.